Observation of hyperfine interaction in photoassociation spectra of ultracold RbYb

C. Bruni and A. Görlitz

Institut für Experimentalphysik, Heinrich-Heine-Universität Düsseldorf, Universitätsstraße 1, 40225 Düsseldorf, Germany

(Received 7 March 2016; published 3 August 2016)

We report on the creation of ultracold heteronuclear and electronically excited Rb*Yb molecules in a hybrid conservative trap by photoassociation of ultracold ^{87}Rb and ^{176}Yb. The molecules are formed below the $Rb_{5p1}(^2P_{1/2}) + Yb_{6s2}(^1S_0)$ dissociation limit and the resonances are detected using trap-loss spectroscopy. By addressing vibrational levels with binding energies down to $E_B = -h \times 2.2\,\mathrm{THz}$, we study the change in hyperfine coupling of the diatomic molecule as a function of internuclear separation. We observe a decreasing hyperfine splitting for more tightly bound excited molecular states where the hyperfine splitting is reduced by more than 30% compared to the atomic value for ^{87}Rb.

DOI: 10.1103/PhysRevA.94.022503

I. INTRODUCTION

The creation and investigation of different species of ultracold molecules and in particular of ultracold heteronuclear molecules have been major goals in experimental atomic physics almost since laser cooling of neutral atoms was first realized experimentally [1–3]. Among the possible applications of ultracold heteronuclear molecules are quantum computation [4] and the experimental realization of complex spin-lattice models [5]. Of particular interest for such applications are heteronuclear molecules with an unpaired electron which possess a magnetic as well as an electric dipole moment in the ground state, thus enhancing the possibilities for manipulation and the study of interactions. While many atomic species have level structures that are amenable to laser cooling, only in very special cases is it possible to laser cool even the simplest diatomic molecules [6–8]. Even then, the efficiency is significantly reduced as compared to laser cooling of atoms.

One of the possibilities to create larger ensembles of ultracold heteronuclear molecules in the electronic ground state is to first laser cool atoms to temperatures in the μK regime and subsequently convert them to molecules. For bialkalis, the most common method for the controlled production of molecules in the electronic ground state (but in highly excited vibrational levels) makes use of so-called magnetic Feshbach resonances [9], thus avoiding coupling to the excited molecular state during the preparation process. Such a strategy for heteronuclear molecules has been successfully implemented so far for KRb [10–12], NaK [13,14], and RbCs [15,16]. For molecular species, such as alkali-metal–alkaline-earth molecules (or electronically similar molecules like RbYb), Feshbach resonances are absent or hard to access experimentally. Thus it is more convenient to produce molecules in the electronic ground state by light-assisted processes which involve coupling of the atomic ground state to the excited molecular state. Such a scheme, which had previously also been demonstrated for bialkalis such as KRb [17], LiCs [18], or RbCs [19], has recently been used to create homonuclear molecules of the alkaline-earth atom strontium [20,21].

In order to devise efficient routes for the light-assisted production of ultracold molecules it is required to have a precise knowledge of the molecular level structure not only of the electronic ground state but also of the excited state. One way to obtain this information is photoassociation (PA) spectroscopy [22] where unbound atoms are coupled to molecular states by using laser light. For RbYb we have previously obtained one- and two-photon photoassociation spectra [23–25] in a double species magneto-optical trap (MOT) at temperatures of a few 100 μK, which provided first insight into the level structure of the electronically excited $^2\Pi_{1/2}$ state of Rb*Yb correlated to the Rb_{5p1} $(^2P_{1/2}) + Yb_{6s2}(^1S_0)$ asymptote. However, for the experimental investigation of RbYb molecules it is eventually required to perform PA in a conservative trap where lower temperatures and higher densities of the atomic ensembles can be achieved, thus improving the conditions for PA. In addition, conservative traps may also be used to trap the molecules once they are produced.

In this paper, we report on PA of RbYb in a combined trapping geometry which involves an optical trap at 555.95 nm for Yb and an almost purely magnetic trap for Rb. At a temperature of a few μK we observe single-photon PA of excited-state molecules with binding energies down to $E_B = -h \times 2.2\,\mathrm{THz}$, thus extending the range of observed molecular binding energies by more than a factor of 2 with respect to our previous work. This allows us to study in more detail the change of the hyperfine coupling of the excited molecular state. First indications of this effect had already been seen in our previous measurements [23,26] and can be verified unambiguously in this paper. The observed modification of the hyperfine coupling originates from a perturbation of the electronic wave function of the Rb atom when approaching the Yb atom. It is hence similar to the mechanism in the ground state of alkali-metal–alkaline-earth molecules which has recently been discussed theoretically in the context of predictions of Feshbach resonances even for this class of ultracold molecules [27–29].

II. EXPERIMENT

In the work presented here, one-photon PA is performed from unbound ground-state atoms, which are confined in a conservative trap, to weakly bound rovibrational levels in a singly excited $^2\Pi_{1/2}$ state of Rb*Yb which is associated to the $Rb_{5p1}(^2P_{1/2}) + Yb_{6s2}(^1S_0)$ atomic dissociation channel (see Fig.1). The isotopic combination which is studied is ^{176}Yb and ^{87}Rb. The hybrid conservative trap (HCT) is building on the trap that we have used to demonstrate sympathetic cooling in a mixture of Rb and Yb [30,31]. This previous

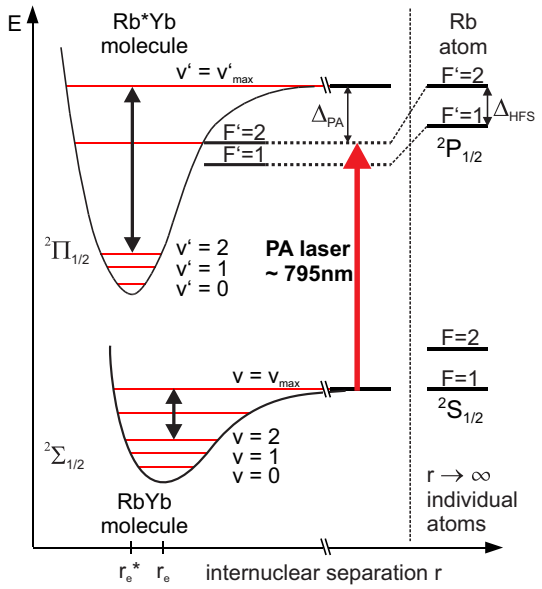

FIG. 1. Relevant level structure (not to scale) in the RbYb molecule. The equilibrium bond lengths of the ground and excited state are denoted as r_e and r_e^* and the vibrational quantum numbers are denoted as v and v′, respectively. For the weakly bound vibrational levels with low rotational quantum number R in the excited $^2\Pi_{1/2}$ state, the coupling of the nuclear spin of the Rb atom to the electronic angular momentum is stronger than the coupling between molecular rotation and the electronic angular momentum. Therefore, the total angular momentum quantum numbers F' corresponding to the atomic states of atomic Rb are also used to indicate the molecular state.

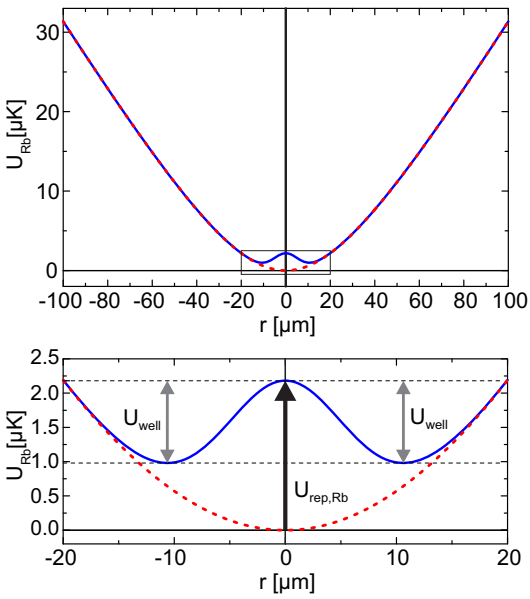

FIG. 2. Modeled trapping potentials for Rb. The pure magnetic trapping potential for Rb (red, dashed) is compared to the combined potential for Rb (blue, solid) which consists of the attractive magnetic potential superimposed on the repulsive ODT potential ODT_{556}. The ODT potential lifts the bottom of the MT by $U_{\mathrm{rep,Rb}} = k_B \times 2.2\,\mu\mathrm{K}$ producing two potential wells with a depth of $U_{\mathrm{well}} = k_B \times 1.2\,\mu\mathrm{K}$. Thus good overlap of the atomic clouds is still assured. The bottom picture shows the relevant section in more detail. The ODT potential for Yb does not get any distortion due to the lack of magnetic moment in the ground state of Yb.

trapping geometry combined a bichromatic optical trap with a magnetic trap for Rb. While it allowed us to observe collisions between the two species, the bichromatic optical potential for Yb, with which it was attempted to minimize the effect on Rb, made it difficult to precisely control the density and overlap of the two species. Therefore, our developed HCT consists of a clover-leaf magnetic trap (MT) for Rb and a single-color near-resonant optical dipole trap at 555.95 nm (ODT_{556}) for Yb tuned close to the $^1S_0 \rightarrow {}^3P_1$ intercombination line at 555.806 nm which is hence red-detuned by only 140 GHz. With a laser power of $P_{556} = 6\,\mathrm{mW}$ at the end of the experimental cycle and a beam waist of $w_{556} = 11\,\mu\mathrm{m}$ this yields a calculated trap depth of $U_{556} = -k_{\mathrm{B}} \times 30\,\mu\mathrm{K}$. Since the natural linewidth of the intercombination line is only 180 kHz and the trap is operated at very low laser power the observed experimental lifetime of optically trapped Yb is several seconds, in agreement with theoretical considerations. While the magnetic field does not affect Yb with its diamagnetic ground state, Rb experiences a light shift in (almost) any optical field. To illustrate the residual effect of the light field of the ODT_{556} on Rb, the modeled total potential for Rb (optical plus magnetic) for the final experimental parameters is shown in Fig. 2. The magnitude of the repulsive optical potential is $U_{\mathrm{rep,Rb}} = k_B \times 2.2\,\mu\mathrm{K}$, resulting in two potential wells with a depth of $U_{\mathrm{well}} = k_B \times 1.2\,\mu\mathrm{K}$ for the total potential. Since the relevant atomic temperatures in the present study are a few μK, this effect does not prevent overlapping of the two atomic clouds. Nevertheless, care has to be taken to align the optical and magnetic fields relative to each other since small deviations still lead to changes in the total potential for Rb.

To prepare an ultracold mixture of Yb and Rb in the HCT, a Yb MOT operating on the $^1S_0 \rightarrow {}^3P_1$ transition at 555.8 nm is first loaded from a Zeeman slower using light tuned close to the $^1S_0 \rightarrow {}^1P_1$ transition at 399 nm. The Yb atoms are then transferred from the MOT to an ODT operating at 1064 nm (ODT_{1064}) yielding a potential depth for Yb of $\approx -k_B \times 350\,\mu\mathrm{K}$ for $P = 4\,\mathrm{W}$ and $w_{1064} = 15\,\mu\mathrm{m}$. The ODT_{1064} creates an approximately five times deeper potential for Rb and hence laser-cooled (but hotter) Rb atoms could easily be captured directly out of a MOT, resulting in heating and loss of the Yb atoms. To avoid this undesired effect, the ODT_{1064} containing the Yb sample is moved out of the vacuum chamber center by translating the focusing lens for the ODT by about 1.6 cm using a motorized stage. Subsequently, a Rb MOT operating on the $^2S_{1/2} \rightarrow {}^2P_{3/2}$ transition can be loaded from a Zeeman slower at approximately the same position as the Yb MOT without affecting the optically trapped Yb atoms. The Rb atoms are then transferred into a clover leaf MT and are further cooled by rf evaporation. To overlap the Rb and Yb clouds, the ODT_{1064} for the Yb atoms is moved back to its initial position which is separated laterally by 1.4 mm from the position of the MT for Rb. Subsequently, the Yb atoms are transferred into the ODT_{556} with an initial power of $P_{556} = 12\,\mathrm{mW}$ achieving a transfer efficiency of >75%. The Rb atoms are then moved to the same position by applying magnetic offset fields to the MT. Just before the two atomic clouds are overlapped,

typically 10^5 Yb atoms at $T_{\mathrm{Yb}} = 12\,\mu$K are trapped in the ODT_{556} beam and roughly 10^7 Rb atoms are spin polarized in the $|F = 1, m_F = -1\rangle$ hyperfine state at $T_{\mathrm{Rb}} = 2\,\mu$K in the MT. After the two atomic clouds are brought into contact, they thermalize to a temperature of $T_{\mathrm{RbYb}} = 2\,\mu$K. With the Rb sample serving as a cold bath, the power for the ODT_{556} can now be decreased to the final value of $P_{556} = 6\,\mathrm{mW}$ without any Yb loss reducing the repulsive potential for Rb for the following PA process. In this configuration, the peak densities for the two species are calculated to be $\rho_{\mathrm{Rb}} = 2.7 \times 10^{13}\,\mathrm{cm}^{-3}$ and $\rho_{\mathrm{Yb}} = 1.1 \times 10^{12}\,\mathrm{cm}^{-3}$, respectively. The described sympathetic cooling process can be exploited to optimize the alignment of the trapping potentials and thus the overlap of the atomic clouds. Since the MT carrying the Rb atoms can easily be shifted by magnetic offset fields, the optimum overlap was determined by minimizing the Yb temperature as a function of the position of the MT for Rb. The alignment procedure was typically performed every day in order to ensure an optimum overlap of the two atomic clouds.

Once the atoms are prepared in the combined HCT, PA spectroscopy is performed by illuminating the atoms with radiation tuned close to the Rb D_1 transition $^2S_{1/2} \rightarrow {}^2P_{1/2}$at 795 nm (wave number $\tilde{\nu}_{\mathrm{D1}} = 12\,579.1037\,\mathrm{cm}^{-1}$). The PA laser radiation is obtained from a tapered amplifier (TA) injected by a homemade external cavity diode laser (ECDL) which yields an output power of 400 mW. After optical alignment and fiber coupling a beam with 100 mW is focused to a waist of $w_0 = 230\,\mu$m corresponding to an intensity of $I = 120\,\mathrm{W/cm}^2$ which irradiates the atoms. To prevent the large amplified spontaneous emission (ASE) background of the TA from resonantly exciting Rb out of the MT, the radiation is spectrally filtered using an interference filter with a full width at half maximum linewidth of 0.4 nm. However, the remaining ASE still prevents us from doing spectroscopy very close to the atomic Rb D_1 line and hence only more deeply bound vibrational levels are investigated here. PA spectroscopy is performed by detecting trap loss as a function of PA laser frequency with a variable exposure time between 10 and 1500 ms. During exposure, the PA laser frequency is ramped over a variable frequency range between 2 and 100 MHz and afterwards the number of remaining atoms for both species is measured by absorption imaging. If the PA laser frequency matches the energy difference between an unbound atom pair in the electronic ground state and a rovibrational level of an electronically excited bound state, excited-state molecules are produced. The created molecules typically decay either into two free atoms with a high kinetic energy or, more likely, into ground-state molecules that can in principle be captured by the HCT. Either way, since only Rb and Yb atoms are detected the formation of molecules results in a loss of atoms from the trap. Due to the mismatch in atom number between the two species by a factor of 100, the PA signal is only observed in the Yb atom number.

The relative vibrational quantum number[1] $\Delta\mathrm{v}' = \mathrm{v}' - \mathrm{v}'_{\mathrm{max}}$ (see Fig. 1 and Table I) is given relative to the vibrational quantum number $\mathbf{v}'_{\mathbf{max}}$ of the most weakly bound level in the electronically excited molecular potential since the exact number of vibrational states in this potential is not yet known. The detuning $\Delta_{\mathrm{PA}} = \tilde{\nu}_{\mathrm{PA}} - \tilde{\nu}_{\mathrm{D1}}$, which is defined by the wave number $\tilde{\nu}_{\mathrm{PA}}$ of the PA laser with respect to the wave number $\tilde{\nu}_{\mathrm{D1}} = 12\,579.1037\,\mathrm{cm}^{-1}$ of the Rb D_1 transition $^2S_{1/2}, F = 1 \rightarrow {}^2P_{1/2}, F' = 2$, is changed for consecutive cycles and measured with a wave meter with an absolute accuracy of $5 \times 10^{-3}\,\mathrm{cm}^{-1}$. In contrast to PA spectroscopy in a MOT, in a conservative trap, the effect of the PA laser cannot be continuously monitored, but each experimental cycle with a duration of ≈ 45 s only yields one value for the trap loss corresponding to a specific frequency (or small frequency interval) of the PA laser radiation. Thus, PA spectroscopy in the HCT is significantly more time consuming and greatly benefits from the knowledge previously obtained from the spectroscopic investigations in the combined MOT [23].

TABLE I. Observed vibrational levels $\Delta\mathrm{v}'$ and corresponding hyperfine splitting Δ_{HFS} in a mixture of ^{87}Rb and ^{176}Yb. The binding energies are given relative to the Rb D_1 transition $^2S_{1/2}, F = 1 \rightarrow {}^2P_{1/2}, F' = 2$ at $\tilde{\nu}_{\mathrm{D1}} = 12\,579.1037\,\mathrm{cm}^{-1}$. Absolute positions have an error of 5×10^{-3} cm^{-1}, and Δ_{HFS} has an estimated error of 30 MHz. No $F' = 1$ component could be observed for the two weak lines $\Delta\mathrm{v}' = -19$ and -24. Here, r_{eff} denotes the calculated internuclear separation from the binding energy for each vibrational level $\Delta\mathrm{v}'$ extrapolated from the molecular rotational constants determined in [23] (see text for further information).

	Δ_{bind} (cm^{-1})		Δ_{HFS}	r_{eff}
$\Delta\mathrm{v}'$	$F' = 2$	$F' = 1$	(MHz)	(in units of a_0)
Rb atom	0	−0.02725	817	∞
−9	−2.7284	−2.7546	785	24.9
−11	−4.8960	−4.9217	772	22.8
−13	−8.0005	−8.0258	762	21.0
−14	−9.9581	−9.9809	686	20.2
−15	−12.1935	−12.2171	708	19.4
−16	−14.8090	−14.8317	693	18.7
−17	−17.6851	−17.7094	710	18.1
−18	−20.9219	−20.9438	678	17.5
−19	−24.5104			16.9
−20	−28.5157	−28.5364	634	16.3
−21	−32.8621	−32.8838	645	15.8
−22	−37.6095	−37.6315	658	15.3
−23	−42.7869	−42.8085	647	14.8
−24	−48.3581			14.4
−25	−54.3464	−54.3662	595	13.9
−26	−60.7819	−60.7993	523	13.5
−27	−67.6306	−67.6495	567	13.1
−28	−74.9147	−74.9330	549	12.7

III. RESULTS

A typical PA scan of the $\Delta\mathrm{v}' = -13$ vibrational level of the electronically excited state of Rb*Yb in the HCT is shown in Fig. 3(a), while Fig. 3(b) shows a spectrum taken in a double-species MOT. From the laser detuning on resonance the binding energy Δ_{bind} of the rovibrational level can be directly inferred. Line shifts stemming from the ODT or the MT potential can be neglected. The two spectral lines that are

[1] In this paper we follow the notation in [23] with $\Delta\mathrm{v}' = 0$ being the most weakly bound state. In contrast, in [25] the vibrational state was labeled by $\mathrm{v} = -\Delta\mathrm{v}' + 1$.

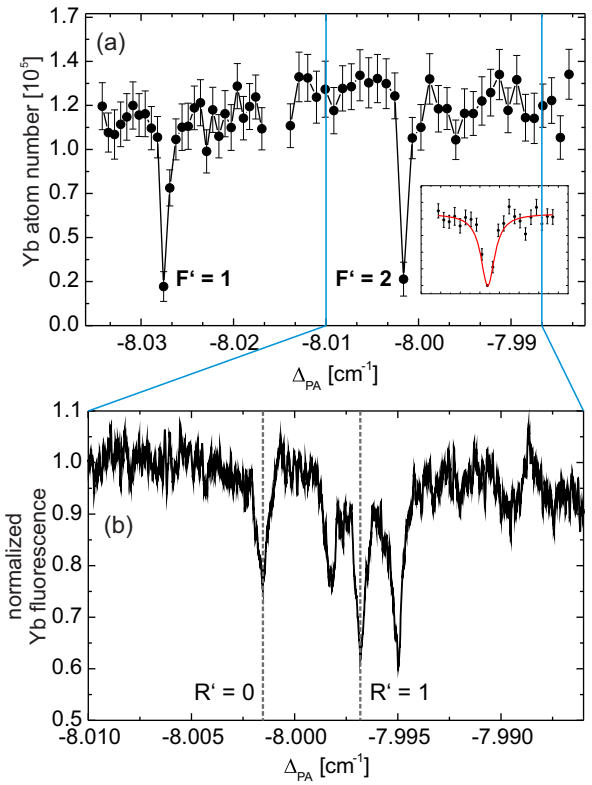

FIG. 3. (a) Typical PA spectrum in the conservative trap showing the vibrational level $\Delta v' = -13$. Each point corresponds to an experimental sequence in which the PA laser frequency is ramped during the PA exposure time by ≈ 30 MHz. The lines connecting adjacent points are just a guide to the eye. The same applies to the Lorentzian fit in the inset, which is a zoom-in of the spectrum with a resolution of ≈ 9 MHz. (b) A typical PA spectrum in combined Rb and Yb MOTs. Here the PA laser frequency is continuously scanned and the Yb MOT fluorescence is detected. Due to higher temperatures in the MOTs higher rotational lines belonging to $R' = 1$ appear and are even more pronounced than the $R' = 0$ line.

observed in the HCT have a separation similar to the hyperfine splitting of the atomic $^2P_{1/2}$ state of ^{87}Rb. In the double-species MOT [Fig. 3(b)], a substructure of these lines is observed which is attributed to molecular rotation in the excited state. From these spectra it can be inferred that for the molecular states investigated here, the coupling of the nuclear spin of the Rb atom to the electronic angular momentum is much stronger than the coupling of the molecular rotation to the electronic angular momentum. Thus, the spectral lines can be described by the quantum numbers $F' = 1$ or 2 corresponding to the Rb atom and a rotational quantum number R'. For $R' > 0$ an additional splitting is observed which is attributed to a coupling between F' and R'. The number of subcomponents is then given by $2X + 1$, where X represents the smaller value of F' and R', respectively. Our experimental observations for the weakly bound vibrational levels agree with Hund's coupling case (e). However, for more deeply bound states this will no longer be true and a direct association of molecular levels with atomic quantum number F' will no longer be valid.

The fact that in the HCT there is only one component corresponding to each of the two quantum numbers $F' = 1$ or 2 is attributed to the low temperature of $\approx 2\,\mu$K. At such a low temperature, collisions between ground-state Rb and Yb atoms are purely s wave since the thermal energy is much less than the height of the centrifugal barrier $E_c = k_B \times 66\,\mu$K for p-wave scattering [22]. Since photoassociation does not change the orbital angular momentum of the atoms, only molecular levels with $R' = 0$ can be excited. In contrast, rotational lines with larger R' can be observed in the combined MOT due to the much higher temperature of $T_{\mathrm{MOT}} = 300\,\mu$K [23].

Performing PA spectroscopy in the HCT, we have been able to detect ten additional vibrational levels of the electronically excited state of Rb*Yb compared to [23], the most tightly bound corresponding to $\Delta v' = -28$. The low duty cycle of the experiment makes it impractical to scan the whole frequency range of ≈ 2.2 THz from the atomic resonance to the most deeply bound vibrational level. We have thus estimated the positions of previously unobserved levels by using local fitting functions to the previously observed levels in the MOT [23]. Following this extrapolation, the vibrational level $\Delta v' = -29$ was predicted to be located at $\Delta_{\mathrm{PA}} = -82.66\,\mathrm{cm}^{-1}$ but no unambiguous resonance was observed, indicating that the corresponding PA transition is rather weak. The predicted position $\Delta_{\mathrm{PA}} = -90.75\,\mathrm{cm}^{-1}$ for the next level $\Delta v' = -30$ is outside the range of the PA laser system.

Table I lists all observed vibrational levels for both total angular momenta $F' = 1$ and 2 of the electronically excited state of Rb*Yb that were observed in this work in the HCT. While most of the vibrational levels from [23] could be reproduced and the binding energies measured within this work agree with the previously reported values, the $\Delta v' = -19$ and 21 levels were found at a 1.3- and 5.8-GHz higher PA laser frequency, respectively. Since the trap-loss signals of the present work in the HCT are unambiguous for both lines and the assumed signal strength in the previous work was just above noise level, we conclude that we have misinterpreted artifacts as lines in [23]. As stated above, due to the ASE of the tapered amplifier, it is more difficult to find weak lines close to the Rb D_1 line in the HCT which makes the spectroscopy of the excited state only feasible for vibrational levels lower than $\Delta v' = -13$, except for the two strong transitions to the levels $\Delta v' = -11$ and -9. The line corresponding to the total angular momentum $F' = 2$ could be observed for all vibrational levels while no unambiguous signal could be obtained for lines corresponding to $F' = 1$ for $\Delta v' = -19$ and -24. This is attributed to a small Franck-Condon overlap between the wave functions of the unbound ground-state atom pair and the vibrational level in the excited state which causes the generally stronger $F' = 2$ line to appear also relatively weak.

Another difference between PA spectroscopy in the combined MOT and in the HCT is that the internal quantum numbers (F, m_F) of ground-state Rb atoms are well defined in the conservative trap since only Rb atoms in the $|F = 1, m_F = -1\rangle$ state are trapped.[2] This also allows us to select specific quantum numbers (F', m'_F) in the excited state of Rb*Yb by the polarization of the PA laser, which is a prerequisite for future experiments aiming at the creation of ground-state

[2]For ^{176}Yb with its diamagnetic ground state all atoms are in the $F_{\mathrm{Yb}} = 0, m_{F,\mathrm{Yb}} = 0$ in the MOT as well as in the HCT.

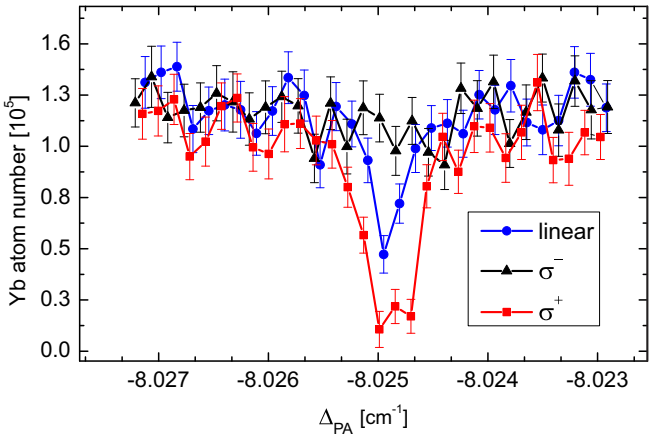

FIG. 4. Polarization dependence of the PA transition to the $F' = 1$ component of the $\Delta v' = -13$ vibrational level. The observed trap loss agrees qualitatively with the relative strength of the dipole matrix elements for the $|F = 1, m_F = -1\rangle \rightarrow |F' = 1\rangle$ transition in Rb which is determined by the angular factors $-1/\sqrt{12}$ for σ^+ polarization and zero for σ^- polarization. Accordingly, the strongest observed transition is driven by σ^+-polarized PA light while, most noticeably, the line vanishes for σ^--polarized light. Due to the magnetic-field geometry in the experiment, linear polarization has to be described as a mixture of σ^+ and σ^- polarization.

molecules in well-defined internal quantum states by means of two-photon PA. In order to verify experimentally that we are able to control which m'_F component is addressed by PA we have investigated the dependence of the $|F = 1, m_F = -1\rangle \rightarrow |F' = 1\rangle$ transition corresponding to the vibrational state $\Delta v' = -13$ on the polarization of the PA laser beam. As displayed in Fig. 4 the observed atom loss depends strongly on the polarization of the PA laser which propagates parallel to the magnetic trap axis and thus the magnetic field, which determines the quantization axis. Qualitatively, these loss features correspond to the relative strength of the dipole matrix elements determined by the angular factors $-1/\sqrt{12}$ for σ^+ polarization, $1/\sqrt{12}$ for π polarization, and zero for σ^- polarization. Since the Rb atoms are in the $|F = 1, m_F = -1\rangle$ level of the atomic ground state, no transition to the $F' = 1$ excited hyperfine level can be driven by σ^--polarized light, while illumination with σ^+ light leads to a maximum of the molecule production and correspondingly the atom loss. Linear polarization which is described as an equal-weight superposition of σ^+ and σ^- polarization in our experimental geometry can excite molecular levels but with reduced efficiency. In contrast, transitions to the $F' = 2$ (not shown in the figure) can be excited with any polarization of the PA laser beam.

In general, excited-state molecules created by PA are loosely bound molecules close to the atomic threshold which hence exhibit physical properties that can be derived from those of their constituent atoms. As a result, the hyperfine structure of photoassociated molecules [see Fig. 3(a)] in such states can be directly related to the hyperfine structure of the atomic Rb D_1 line which has a splitting of $\Delta_{\mathrm{HFS}} = 817\,\mathrm{MHz}$ [32] between the $F' = 2$ and 1 levels. As stated in Table I and has been observed in [23], the hyperfine splitting of the most weakly bound vibrational levels of Rb*Yb is very close to the atomic value while it decreases significantly as the levels become more tightly bound reaching a value of 549(30) MHz for the $\Delta v' = -28$ level with a binding energy of $E_B = -h \times 2.2\,\mathrm{THz}$, which is the most deeply bound level that we were able to detect. In essence the observed behavior displays the transition from the limit of separated atoms over loosely bound to more tightly bound molecular states. While an accurate theoretical description of the variation of the hyperfine splitting with internuclear distance r goes beyond the scope of this paper, a first simplified description is outlined below.

The hyperfine structure of an atom results from the interaction between its nuclear spin and the angular momentum of the electrons. In the PA experiments presented in this paper, the involved excited state of Rb is the $^2P_{1/2}$ state. In this case, the dominant contribution to the hyperfine coupling is due to the dipole-dipole interaction between the nuclear and electron magnetic moments and the hyperfine coupling constant can be described as

$$A_{\mathrm{dd}} = \frac{\mu_0}{4\pi} g_N\, \mu_{\mathrm{N}}\, g_e\, \mu_{\mathrm{B}} \left\langle \frac{1}{r^3} \right\rangle \langle 3\cos^2\theta - 1\rangle, \qquad (1)$$

where g_e and g_N are the electronic and nuclear Landé g factors and μ_{B} and μ_{N} are the Bohr and nuclear magnetons. The $\langle ... \rangle$ brackets indicate an average over the electronic wave function. In the case of the $^2P_{1/2}$ state of an unperturbed ^{87}Rb atom, the hyperfine coupling constant has a value of $A_{^2\mathrm{P}_{1/2}} = h \times 408.328\,\mathrm{MHz}$ [32] leading to an atomic hyperfine splitting of $\Delta E_{\mathrm{HFS}} = 2\, A_{^2\mathrm{P}_{1/2}} = h \times 817\,\mathrm{MHz}$.

As the mean distance between the constituent atoms of the Rb*Yb molecule is reduced and the binding energy is increased, the electronic wave function of the Rb atom is perturbed due to the presence of the Yb atom. This in turn alters the hyperfine coupling constant $A_{^2\mathrm{P}_{1/2}}$ leading to a modification of the hyperfine splitting as a function of internuclear separation r. Figure 5 shows the measured hyperfine splitting $\Delta_{\mathrm{HFS}} = \Delta E_{\mathrm{HFS}}/h$ as a function of effective internuclear

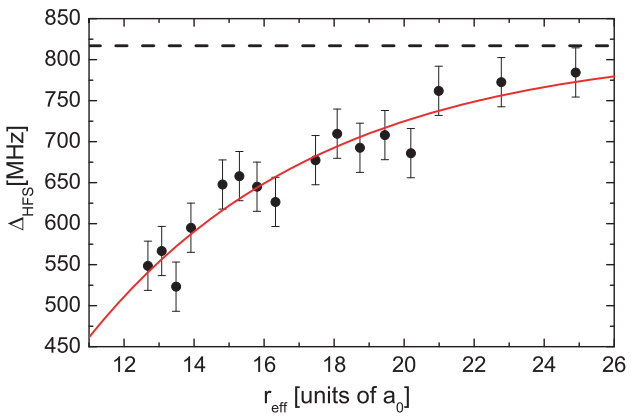

FIG. 5. Measured hyperfine splitting in molecular Rb*Yb as a function of effective internuclear separation r_{eff}. The horizontal dashed line indicates the hyperfine splitting of $\Delta_{\mathrm{HFS}} = 817\,\mathrm{MHz}$ in the $^2P_{1/2}$ state of atomic Rb. The solid red curve is a simple exponential fit to guide the eye. A decrease in Δ_{HFS} with decreasing r_{eff} is apparent showing a variation of the hyperfine coupling constant of the Rb atom due to the presence of the Yb atom and hence a gradual passage to more tightly bound Rb*Yb molecules.

separation r_{eff} where the horizontal dashed line represents the atomic hyperfine splitting of $\Delta_{\mathrm{HFS}} = 817\,\mathrm{MHz}$. The values for r_{eff} (see also Table I) were deduced up to the vibrational level $\Delta v' = -18$ from the molecular rotational constants determined in [23] assuming the molecule to be a fixed rotator. Values of r_{eff} for more deeply bound vibrational levels have been obtained by extrapolating from the known values assuming a power-law potential. Thus, r_{eff} was correlated to the binding energy of each vibrational state $\Delta v'$ since the rotational energy of the molecule could not be directly measured. The deepest observed bound vibrational state belongs to $\Delta v' = -28$ and exhibits a hyperfine splitting of 549(30) MHz which is already less than 70% of the atomic splitting. It is worth noting that the effect that we observe here in the excited state of Rb*Yb is closely related to an effect that has been proposed to lead to observable Feshbach resonances in RbYb and alkali-metal–alkaline-earth molecules [27–29].

IV. CONCLUSION

In conclusion, we have successfully produced ultracold excited Rb*Yb molecules in a hybrid conservative trap at a temperature of $2\,\mu\mathrm{K}$ and determined the binding energies of vibrational levels down to $\Delta v' = -28$ with a binding energy of $E_B = -h \times 2.2\,\mathrm{THz}$. In this study we were able to add several levels that had not been observed previously and correct two previously misidentified values for binding energies. We have demonstrated that in the conservative trap we are able to control all internal quantum states of the molecule. In addition, we have observed a significant deviation of the hyperfine splitting in more deeply bound vibrational levels of Rb*Yb from the atomic value for Rb. The results presented here not only add to our knowledge of the structure of RbYb but also constitute an important step towards the production of ultracold RbYb ground-state molecules since the improved experimental methods for combined trapping of Rb and Yb will be beneficial also for further experimental studies. Combining the results presented here with the methods applied for two-photon spectroscopy of the ground state [24,25] will be a good starting point to finally create ground-state molecules.

ACKNOWLEDGMENTS

We thank Tobias Franzen and Nils Nemitz for discussions and careful reading of the manuscript.

[1] S. Chu, Rev. Mod. Phys. **70**, 685 (1998).
[2] W. D. Phillips, Rev. Mod. Phys. **70**, 721 (1998).
[3] C. N. Cohen-Tannoudji, Rev. Mod. Phys. **70**, 707 (1998).
[4] D. DeMille, Phys. Rev. Lett. **88**, 067901 (2002).
[5] G. K. Brennen, A. Micheli, and P. Zoller, New J. Phys. **9**, 138 (2007).
[6] J. F. Barry, E. S. Shuman, E. B. Norrgard, and D. DeMille, Phys. Rev. Lett. **108**, 103002 (2012).
[7] J. F. Barry, D. J. McCarron, E. B. Norrgard, M. H. Steinecker, and D. DeMille, Nature (London) **512**, 286 (2014).
[8] D. J. McCarron, E. B. Norrgard, M. H. Steinecker, and D. DeMille, New J. Phys. **17**, 035014 (2015).
[9] T. Köhler, K. Góral, and P. S. Julienne, Rev. Mod. Phys. **78**, 1311 (2006).
[10] C. Ospelkaus, S. Ospelkaus, L. Humbert, P. Ernst, K. Sengstock, and K. Bongs, Phys. Rev. Lett. **97**, 120402 (2006).
[11] K.-K. Ni, S. Ospelkaus, M. H. G. de Miranda, A. Pe'er, B. Neyenhuis, J. J. Zirbel, S. Kotochigova, P. S. Julienne, D. S. Jin, and J. Ye, Science **322**, 231 (2008).
[12] S. A. Moses, J. P. Covey, M. T. Miecnikowski, B. Yan, B. Gadway, J. Ye, and D. S. Jin, Science **350**, 659 (2015).
[13] C.-H. Wu, J. W. Park, P. Ahmadi, S. Will, and M. W. Zwierlein, Phys. Rev. Lett. **109**, 085301 (2012).
[14] J. W. Park, S. A. Will, and M. W. Zwierlein, Phys. Rev. Lett. **114**, 205302 (2015).
[15] T. Takekoshi, M. Debatin, R. Rameshan, F. Ferlaino, R. Grimm, H.-C. Nägerl, C. R. Le Sueur, J. M. Hutson, P. S. Julienne, S. Kotochigova, and E. Tiemann, Phys. Rev. A **85**, 032506 (2012).
[16] M. P. Köppinger, D. J. McCarron, D. L. Jenkin, P. K. Molony, H.-W. Cho, S. L. Cornish, C. R. Le Sueur, C. L. Blackley, and J. M. Hutson, Phys. Rev. A **89**, 033604 (2014).
[17] K. Aikawa, D. Akamatsu, M. Hayashi, K. Oasa, J. Kobayashi, P. Naidon, T. Kishimoto, M. Ueda, and S. Inouye, Phys. Rev. Lett. **105**, 203001 (2010).
[18] J. Deiglmayr, A. Grochola, M. Repp, K. Mörtlbauer, C. Glück, J. Lange, O. Dulieu, R. Wester, and M. Weidemüller, Phys. Rev. Lett. **101**, 133004 (2008).
[19] J. M. Sage, S. Sainis, T. Bergeman, and D. DeMille, Phys. Rev. Lett. **94**, 203001 (2005).
[20] S. Stellmer, B. Pasquiou, R. Grimm, and F. Schreck, Phys. Rev. Lett. **109**, 115302 (2012).
[21] G. Reinaudi, C. B. Osborn, M. McDonald, S. Kotochigova, and T. Zelevinsky, Phys. Rev. Lett. **109**, 115303 (2012).
[22] K. M. Jones, E. Tiesinga, P. D. Lett, and P. S. Julienne, Rev. Mod. Phys. **78**, 483 (2006).
[23] N. Nemitz, F. Baumer, F. Münchow, S. Tassy, and A. Görlitz, Phys. Rev. A **79**, 061403(R) (2009).
[24] F. Münchow, C. Bruni, M. Madalinski, and A. Görlitz, Phys. Chem. Chem. Phys. **13**, 18734 (2011).
[25] M. Borkowski, P. S. Żuchowski, R. Ciuryło, P. S. Julienne, D. Kędziera, Ł. Mentel, P. Tecmer, F. Münchow, C. Bruni, and A. Görlitz, Phys. Rev. A **88**, 052708 (2013).
[26] N. Nemitz, Ph.D. thesis, Heinrich-Heine-Universität Düsseldorf, 2008.
[27] P. S. Żuchowski, J. Aldegunde, and J. M. Hutson, Phys. Rev. Lett. **105**, 153201 (2010).
[28] D. A. Brue and J. M. Hutson, Phys. Rev. Lett. **108**, 043201 (2012).
[29] D. A. Brue and J. M. Hutson, Phys. Rev. A **87**, 052709 (2013).
[30] S. Tassy, N. Nemitz, F. Baumer, C. Höhl, A. Batär, and A. Görlitz, J. Phys. B. **43**, 205309 (2010).
[31] F. Baumer, F. Münchow, A. Görlitz, S. E. Maxwell, P. S. Julienne, and E. Tiesinga, Phys. Rev. A **83**, 040702 (2011).
[32] G. P. Barwood, P. Gill, and W. R. C. Rowley, Appl. Phys. B **53**, 142 (1991).